

# Synthesis and photocatalytic property of Prussian blue/g-C<sub>3</sub>N<sub>4</sub> composite applied to degradation of rhodamine B under visible light

Thi Thuy Trang Phan, Thi Kim Khuu Huynh, Chieu Dong Ho Nguyen, Thi Thanh Nu Nguyen, Hoai Na Ho Nguyen, Thi Hoa Ly Nguyen, Lan Nguyen Thi\*

Faculty of Science, Quy Nhon University, 170 An Duong Vuong St., Quy Nhon, Vietnam

\* Correspondence to Lan Nguyen Thi <nguyenthilan@qnu.edu.vn>

(Received: 12 April 2022; Accepted: 14 May 2022)

**Abstract.** In this work, the Prussian blue/g-C<sub>3</sub>N<sub>4</sub> (PB/g-C<sub>3</sub>N<sub>4</sub>) composite was synthesized from Prussian blue and g-C<sub>3</sub>N<sub>4</sub> via a simple method. The composite was characterized by using X-ray diffraction, Fourier-transform infrared spectroscopy, and ultraviolet-visible diffuse reflectance spectroscopy. The material's photocatalytic performance was studied via the degradation of rhodamine B (RhB). The results show that the composite degraded RhB more than pristine Prussian blue under visible light after 60 min. This material is promising for organic waste treatment.

**Keywords:** RhB, Prussian blue, g-C<sub>3</sub>N<sub>4</sub>

## 1 Introduction

Rapid development of science and technology leads to the discharge of various new chemicals into wastewater. Those harmful contaminants could consecutively affect humans' health through food chains and accumulate until severe diseases. Therefore, investigations on water purification or reducing toxic pollutants in released wastewater are urgent efforts of the scientific and industrial community.

Currently, different techniques are applied to treat water sources, such as adsorption [1] reverse osmosis [2], and microbiological treatment [3]. These techniques are usually expensive and insufficient. Recently, photocatalysis based on semiconductors has been considered an effective and promising method to replace traditional ones for treating organic substances in aqueous media. Heterogeneous photocatalysis belongs to the advanced oxidation processes group with numerous advantages, such as the reaction

occurring at standard temperature and pressure conditions [4]. It can take advantage of sunlight and organic compounds. Organic matter is broken down into CO<sub>2</sub>, H<sub>2</sub>O, and other inorganic substances. One of the new research directions is the application of the Fenton reaction in the photocatalysis process to treat toxic organic wastes that are difficult to decompose in the aquatic environment, such as pharmaceuticals and antibiotics, because this method has a low cost, simple operation, mild reaction conditions [5, 6], and high efficiency [7]. The Fenton reaction involves the formation of •OH through the decomposition of H<sub>2</sub>O<sub>2</sub>. Free radicals with high oxidising activity quickly decompose organic compounds into harmless inorganic compounds. Prussian blue (PB), a representative of metal-organic framework compounds with a face-centred cubic arrangement, is constructed of Fe<sup>2+</sup> and Fe<sup>3+</sup> alternatively coordinated with C≡N cyanide bridges [8]. Since its low cost and harmlessness to the environment, PB was

reported as an effective catalyst for the heterogeneous photo-Fenton reaction [9, 10]. Because of its porous structure, PB is favourable for the mass transfer process [11]. In addition, as an electron mediator, PB is a promising co-catalyst to improve electron transport in the photo-Fenton catalytic process of the  $\text{Fe}_2\text{O}_3$ @polypyrrole composite [12]. The improvement of photo-Fenton-catalytic performance is achieved by enhancing the generation of electrons, which are considered reductive agents for reversibility of  $\text{Fe}^{2+}/\text{Fe}^{3+}$ . This has been demonstrated via coupling Fenton's active catalyst with a photo-semiconductor to form a composite material [13-15]. Recently, g- $\text{C}_3\text{N}_4$  has attracted much attention for its photocatalyst applications in water splitting [16, 17] and decompose organic pollutants [18, 19] under visible light. This material has numerous advantages, such as a bandgap of about 2.7 eV, the possibility of a large-scale production, and non-toxicity [20]. However, pure g- $\text{C}_3\text{N}_4$  exhibits a fast recombination rate of photoelectron and hole pairs [21].

In this work, we report a synthesis of PB decorated on g- $\text{C}_3\text{N}_4$  using a facile solid-vapor reaction. Under visible light, the catalyst exhibits highly effective degradation of organic pollutants (using Rhodamine B as an exemplary compound). Therein, the heterojunction formed between g- $\text{C}_3\text{N}_4$  (an electron donor) and PB (a heterogeneous Fenton-like catalyst) provides an effective pathway for charge transport, leading to significantly improved photocatalytic-Fenton-like performance

## 2 Experimental

### 2.1 Material synthesis

Chemicals: All chemicals for materials synthesis, including sodium ferrocyanide decahydrate ( $\text{Na}_4\text{Fe}(\text{CN})_6$ ,  $\geq 99\%$ ), hydrochloric acid (HCl, 37%),

urea ( $\text{CO}(\text{NH}_2)_2$ ,  $\geq 99\%$ ), and rhodamine B (RhB), were purchased from Sigma-Aldrich and used directly without further purification.

Materials synthesis: Pure g- $\text{C}_3\text{N}_4$  was prepared from urea with the solid-state decomposition and condensation method. Typically, well-ground urea powder was transferred to an alumina crucible covered with aluminum foil and calcinated at 550 °C in the air for one hour with a rising rate of 10 degrees per minute. The obtained solid product was re-ground and denoted as CN.

For synthesizing the composites of PB and CN, 0.1 g of as-prepared CN was well-dispersed to 100 mL of a 0.3 mol·L<sup>-1</sup>  $\text{Na}_4\text{Fe}(\text{CN})_6$  solution under continuous stirring for 12 h. After that, the solid was collected with centrifugation and dried at 80 °C overnight. The reactor was constructed from two vials with diameters of 1.4 and 3.2 cm, wherein the small vial was put entirely inside the other. The obtained solid was transferred to the large vial, while the small vial was filled with concentrated hydrochloric acid (1 mL). Subsequently, the reactor was sealed and aged at ambient temperature for 24 hours. After the reaction was completed, the solid powder turned from yellow white to light blue. The sample was then rinsed thoroughly with deionized water and ethanol three times before drying at 80 °C. The obtained product was denoted as 0.3-H-PB/CN. The pure PB was also prepared in the same procedure directly from  $\text{Na}_4\text{Fe}(\text{CN})_6$  precursor the and hydrochloric acid. The dark-blue solid was rinsed with ethanol, dried at 80 °C, and denoted as H-PB.

### 2.2 Material characterization

The phase structure information of the as-prepared samples was determined with X-ray diffraction (XRD) analysis conducted on a Rigaku X-ray diffractometer with Cu-K $\alpha$  radiation ( $\lambda =$

1.5406 Å) at an accelerating voltage of 45 kV and a current of 200 mA with a scanning step of 0.02° in a 2θ range of 10–80°. In addition, the Rietveld refinement was performed by using GSAS software. The Fourier-transform infrared (FT-IR) spectroscopy was carried out on a Shimadzu IR Prestige-21 spectrophotometer with a sample concentration of 1% in weight in KBr pellets. The Kubelka-Munk equation for the optical bandgap of the as-prepared samples was obtained from ultraviolet-visible diffuse reflectance spectroscopy (UV-Vis DRS) data, which were recorded on a Shimadzu UV-2600 spectrophotometer equipped with a spherical diffuse reflectance accessory.

### 2.3 Photo-Fenton catalytic properties

The photo-Fenton catalytic activity of the as-prepared samples was investigated via the degradation of RhB. 50 mg of catalyst was dispersed in a 100 mL of the RhB solution with an initial concentration of 30 mg·L<sup>-1</sup>. Then, the dispersion was kept in the dark under continuous stirring for one hour to achieve the adsorption-desorption equilibrium. In the next step, 200 μL of a 30% H<sub>2</sub>O<sub>2</sub> solution (corresponding to 0.02 mol·L<sup>-1</sup> in final concentration) was added. Finally, the dispersion was exposed to irradiation of a 60 W-incandescent lamp with a UV cut-off filter. Every 10 minutes, 10 mL of dispersion was withdrawn and centrifuged to eliminate the catalyst. The RhB concentration was determined by measuring the intensity of the maximum absorption peak at a wavelength of 553 nm on an Optizen Pop-S UV-Vis spectrophotometer.

## 3 Results and discussions

Fig. 1 shows the XRD patterns of CN, H-PB, and 0.3-H-PB/CN. For the XRD pattern of CN, the two conspicuous diffractions are observed at 13.1 and 27.3°, coinciding with the intralayer *d*-spacing of the (100) plane and interlayer packing of the

aromatic tri-s-triazine (200) plane [22]. Meanwhile, the diffraction peaks at 17.4, 24.7, 35.3, 39.5, 43.4, 50.7, 54.2, and 57.2° in the XRD patterns of H-PB, corresponding to the (100), (110), (200), (210), (211), (220), (300), and (310) planes, are well matched to the face-centred cubic phase of Fe<sub>4</sub>[Fe(CN)<sub>6</sub>]<sub>3</sub> (JCPDS No. 01-0239).

As a combination, the 0.3-H-PB/CN composite shows an XRD pattern similar to the XRD patterns of the components. The diffraction peaks of both g-C<sub>3</sub>N<sub>4</sub> and PB phases are observable. Remarkably, the intensity of peaks regarded as the cubic phase of PB in the composites increases with the escalation of Na<sub>4</sub>Fe(CN)<sub>6</sub> precursor concentration. This could be assigned to the predominant content of PB over CN in the composites.

To identify the presence of the bonds and functional groups of the synthesized samples, we recorded their FT-IR spectra. As shown in Fig. 2, the FT-IR spectrum of g-C<sub>3</sub>N<sub>4</sub> exhibits a broadband from 3655 to 2922 cm<sup>-1</sup>, representing partly hydrogenated nitrogen groups (-NHS). Meanwhile, the signals at a wavenumber range of 1400–1670 cm<sup>-1</sup> could be attributed to the stretching mode of the C=N and C-N bonds in the aromatic rings of heptazine units [12]. The absorption peaks in a range of 1090–1340 cm<sup>-1</sup> are assigned to the vibration of C-NH-C, an imperfect version of ternary bridge N-(C)<sub>3</sub> in the melam structure [4].

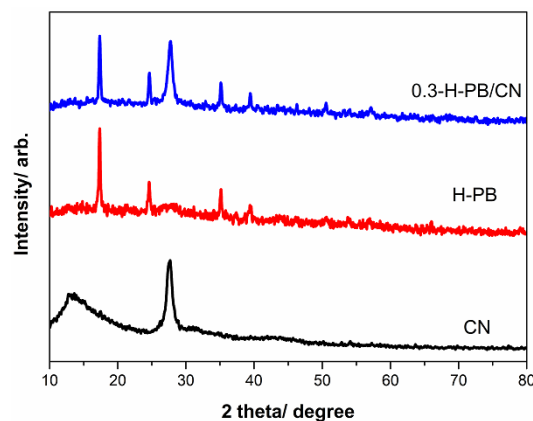


Fig. 1. XRD patterns of CN, H-PB, and 0.3-H-PB/CN

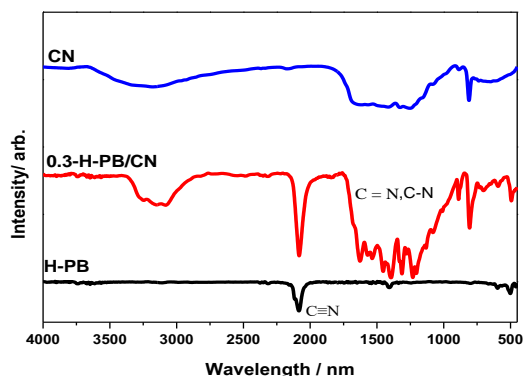


Fig. 2. FT-IR spectra of CN, H-PB, and 0.3-H-PB/CN

The absorption peak at  $801\text{ cm}^{-1}$  could characterize the out-of-plane bending mode of aromatic heterocyclic triazine units, while the bending mode of the primary amine group is related to the absorption peak at  $890\text{ cm}^{-1}$ . Besides, the strong absorption peak at  $2081\text{ cm}^{-1}$  could be assigned to the stretching vibration of the  $\text{C}\equiv\text{N}$  cyanide group in the  $\text{Fe}^{2+}\text{-C}\equiv\text{N-Fe}^{3+}$  units of the PB structure. In addition, the signals in the far-infrared region at  $498$  and  $595\text{ cm}^{-1}$  are ascribed to the bending mode of  $\text{Fe}^{\text{II}}$  and  $\text{Fe}^{\text{III}}$  binding to the  $\text{C}\equiv\text{N}$  group. Furthermore, the strange peak located at the wavenumber of  $1411\text{ cm}^{-1}$  could be attributed to the asymmetric stretching mode of  $\text{N-H}$  in ammonium ions which could be formed via the partial decomposition of the  $\text{C}\equiv\text{N}$  group during the synthesis reaction [23].

From Fig. 3, it can be seen that the obtained H-PB and 0.3-H-PB/CN samples have an absorption shift in the visible light region compared with the CN sample. To determine the band gap, we analyzed the UV-Vis DRS data by using the Kubelka–Munk equation presented in Fig. 4. Accordingly, the bandgap values of CN, H-PB, and edge components of the odd PB and  $g\text{-C}_3\text{N}_4$  in the 0.3-H-PB/CB mixture are 2.72, 1.79, 1.86, and 2.59 eV, respectively.

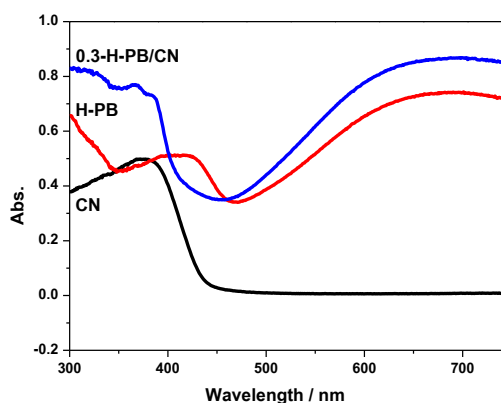


Fig. 3. UV-Vis DRS spectra of CN, H-PB, and 0.3-H-PB/CN

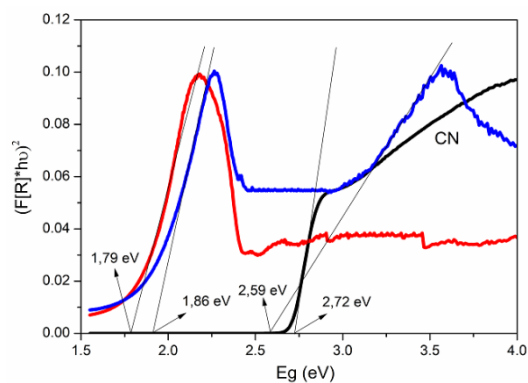


Fig. 4. Kubelka–Munk plot derived from UV-Vis DRS spectra of CN, H-PB, and 0.3-H-PB/CN

The photo-Fenton catalytic activity of as-prepared samples was examined with the decomposition of RhB.

Fig. 5 shows the degradation of RhB by time under photo-oxidation photocatalytic of CN and 0.3-H-PB/CN and the Fenton reaction of H-PB. The efficiency of the photo-Fenton activity of H-PB and the photo-Fenton-like reaction of the CN is improved but insufficient for practical application. Meanwhile, the combination of the PB and  $g\text{-C}_3\text{N}_4$  phase in composites significantly enhances the photo-Fenton catalytic decomposition of RhB. Specifically, 0.3-H-PB/CN exhibits an 89.2% degradation efficiency after 30 min and 94.1% after 60 min of reaction.

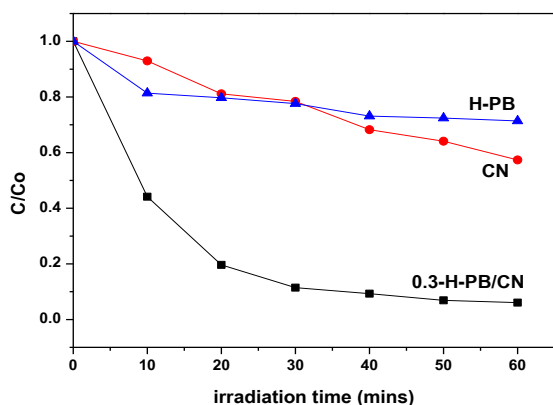


Fig. 5. Photo-Fenton catalytic activity of CN, H-PB, and 0.3-H-PB/CN

In addition, the kinetic feature of the RhB degradation with different catalysts and reaction conditions was investigated by using the pseudo-first-order kinetic model. Accordingly, the 0.3-H-PB/CN catalyst exhibits the highest reaction rate ( $0.046 \text{ min}^{-1}$ ), ten times higher than H-PB. This indicates that the addition of  $g\text{-C}_3\text{N}_4$  leads to significant improvement in the photo-Fenton catalytic activity of pure PB.

The enhancement in the photo-Fenton catalytic performance of the PB/ $g\text{-C}_3\text{N}_4$  composite could be attributed to the synergic effect of its components. As a photo-active semiconductor,  $g\text{-C}_3\text{N}_4$  could provide adequately reductive electron for  $\text{Fe}^{3+}$  reduction in the Fenton reaction of PB. Meanwhile, the heterojunction formed between

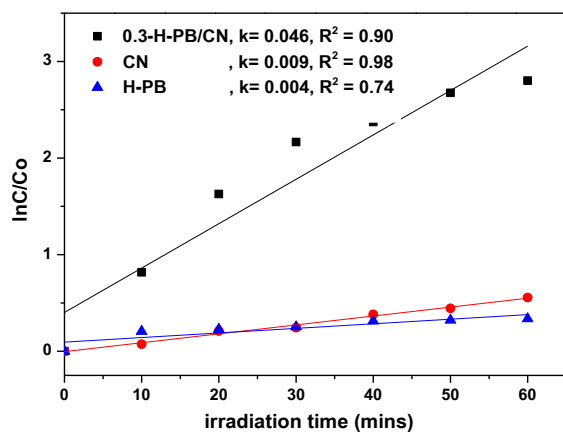


Fig. 6. Kinetic fitting plot using the pseudo-first-order model of CN, H-PB, and 0.3-H-PB/CN

$g\text{-C}_3\text{N}_4$  and PB could induce a suitable charge transport to increase the lifetime of photo-generated charge carriers of individual semiconductors.

## 4 Conclusion

In this study, a facile solid-state reaction at ambient temperature was reported as a successful method for synthesizing PB and its composite with  $g\text{-C}_3\text{N}_4$ . The obtained composites exhibit excellent photo-Fenton catalytic performance under visible irradiation. The 0.3-H-PB/CN sample gave the highest RhB decomposition efficiency of 94.1% after 60 minutes of reaction with  $200 \mu\text{L H}_2\text{O}_2$ . The bandgap value of 0.3-H-PB/CN with individual components is 1.86 and 2.59 eV. This is one of the research directions on materials with potential applications in water environment treatment.

## Funding statement

This research was funded by Faculty of Natural Sciences, Quy Nhon University, in the student scientific research project under code S2021.708.09.

## References

1. Rashid R, Shafiq I, Akhter P, Iqbal MJ, Hussain M. A state-of-the-art review on wastewater treatment techniques: the effectiveness of adsorption method. *Environmental Science and Pollution Research*. 2021;28(8):9050-66.
2. Umar M, Roddick F, Fan L. Recent Advancements in the Treatment of Municipal Wastewater Reverse Osmosis Concentrate—An Overview. *Critical Reviews in Environmental Science and Technology*. 2015;45(3):193-248.
3. Dadrasnia A, Usman M, Kang T, Velappan R, Shahsavari N, Vejan P, et al. Microbial Aspects in Wastewater Treatment – A Technical Review. *Environmental Pollution and Protection*. 2017;2:75-84.

4. Mushtaq MA, Arif M, Yasin G, Tabish M, Kumar A, Ibraheem S, et al. Recent developments in heterogeneous electrocatalysts for ambient nitrogen reduction to ammonia: Activity, challenges, and future perspectives. *Renewable and Sustainable Energy Reviews*. 2023;176:113197.
5. Brillas E. Fenton, photo-Fenton, electro-Fenton, and their combined treatments for the removal of insecticides from waters and soils. A review. *Separation and Purification Technology*. 2022;284:120290.
6. Guo J, Zhang A, Pei Z, Liu X, Xu B, Jia H. Efficient photo-Fenton degradation performance, mechanism, and pathways of tetracycline hydrochloride over missing-linker metal-organic framework with mix-valence coordinatively unsaturated metal sites. *Separation and Purification Technology*. 2022;287:120568.
7. Shen Y, Zhou Y, Zhang Z, Xiao K. Cobalt-copper oxalate nanofibers mediated Fenton degradation of Congo red in aqueous solutions. *Journal of Industrial and Engineering Chemistry*. 2017;52:153-61.
8. Xiao J, Lai J, Li R, Fang X, Zhang D, Tsiakaras P, et al. Enhanced Ultrasonic-Assisted Heterogeneous Fenton Degradation of Organic Pollutants over a New Copper Magnetite (Cu-Fe<sub>3</sub>O<sub>4</sub>/Cu/C) Nanohybrid Catalyst. *Industrial & Engineering Chemistry Research*. 2020;59(27):12431-40.
9. Wang N, Ma W, Du Y, Ren Z, Han B, Zhang L, et al. Prussian Blue Microcrystals with Morphology Evolution as a High-Performance Photo-Fenton Catalyst for Degradation of Organic Pollutants. *ACS Applied Materials & Interfaces*. 2019;11(1):1174-84.
10. Tong X, Jia W, Li Y, Yao T, Wu J, Yang M. One-step preparation of reduced graphene oxide/Prussian blue/polypyrrole aerogel and their enhanced photo-Fenton performance. *Journal of the Taiwan Institute of Chemical Engineers*. 2019;102:92-8.
11. Lin H, Fang Q, Wang W, Li G, Guan J, Shen Y, et al. Prussian blue/PVDF catalytic membrane with exceptional and stable Fenton oxidation performance for organic pollutants removal. *Applied Catalysis B: Environmental*. 2020;273:119047.
12. Yang Y, Ma S, Qu J, Li J, Liu Y, Wang Q, et al. Transforming type-II Fe<sub>2</sub>O<sub>3</sub>@polypyrrole to Z-scheme Fe<sub>2</sub>O<sub>3</sub>@polypyrrole/Prussian blue via Prussian blue as bridge: Enhanced activity in photo-Fenton reaction and mechanism insight. *Journal of Hazardous Materials*. 2021;405:124668.
13. Li K, Liang Y, Yang H, An S, Shi H, Song C, et al. New insight into the mechanism of enhanced photo-Fenton reaction efficiency for Fe-doped semiconductors: A case study of Fe/g-C<sub>3</sub>N<sub>4</sub>. *Catalysis Today*. 2021;371:58-63.
14. Jiang J, Gao J, Li T, Chen Y, Wu Q, Xie T, et al. Visible-light-driven photo-Fenton reaction with  $\alpha$ -Fe<sub>2</sub>O<sub>3</sub>/BiOI at near neutral pH: Boosted photogenerated charge separation, optimum operating parameters and mechanism insight. *Journal of Colloid and Interface Science*. 2019;554:531-43.
15. Li X, Wang J, Rykov AI, Sharma VK, Wei H, Jin C, et al. Prussian blue/TiO<sub>2</sub> nanocomposites as a heterogeneous photo-Fenton catalyst for degradation of organic pollutants in water. *Catalysis Science & Technology*. 2015;5(1):504-14.
16. Chen X, Shi R, Chen Q, Zhang Z, Jiang W, Zhu Y, et al. Three-dimensional porous g-C<sub>3</sub>N<sub>4</sub> for highly efficient photocatalytic overall water splitting. *Nano Energy*. 2019;59:644-50.
17. Wu C, Xue S, Qin Z, Nazari M, Yang G, Yue S, et al. Making g-C<sub>3</sub>N<sub>4</sub> ultra-thin nanosheets active for photocatalytic overall water splitting. *Applied Catalysis B: Environmental*. 2021;282:119557.
18. Kang Z, Ke K, Lin E, Qin N, Wu J, Huang R, et al. Piezoelectric polarization modulated novel Bi<sub>2</sub>WO<sub>6</sub>/g-C<sub>3</sub>N<sub>4</sub>/ZnO Z-scheme heterojunctions with g-C<sub>3</sub>N<sub>4</sub> intermediate layer for efficient piezophotocatalytic decomposition of harmful organic pollutants. *Journal of Colloid and Interface Science*. 2022;607:1589-602.
19. Chen Z, Zhang S, Liu Y, Alharbi NS, Rabah SO, Wang S, et al. Synthesis and fabrication of g-C<sub>3</sub>N<sub>4</sub>-based materials and their application in elimination of pollutants. *Science of The Total Environment*. 2020;731:139054.
20. Al-Ahmed A. Photocatalytic properties of graphitic carbon nitrides (g-C<sub>3</sub>N<sub>4</sub>) for sustainable green hydrogen production: Recent advancement. *Fuel*. 2022;316:123381.
21. Fu J, Yu J, Jiang C, Cheng B. g-C<sub>3</sub>N<sub>4</sub>-Based heterostructured photocatalysts, *Advanced Energy Materials*. 2018;8(3):1701503.
22. Fina F, Callear SK, Carins GM, Irvine JTS. Structural Investigation of Graphitic Carbon

- Nitride via XRD and Neutron Diffraction. Chemistry of Materials. 2015;27(7):2612-8.
23. He X, Tian L, Qiao M, Zhang J, Geng W, Zhang Q. A novel highly crystalline  $\text{Fe}_4(\text{Fe}(\text{CN})_6)_3$  concave cube anode material for Li-ion batteries with high capacity and long life. Journal of Materials Chemistry A. 2019;7(18):11478-86.